International Journal of Technology v(i) pp-pp (YYYY)
Received ……..../ Revised …….. / Accepted ……

International Journal of Technology

http://ijtech.eng.ui.ac.id

Facile and Sustainable Arc Plasma Assisted Synthesis of Mesoporous Carbon: Characterization and Its Application as a CO_2 Adsorbent

Abstract. Increasing CO_2 concentrations in the atmosphere have an impact on rising temperatures and climate change. CO_2 separation through the adsorption process is an attractive option due to its low energy consumption and installation costs. Activated carbon was chosen as an adsorbent because it has better CO_2 adsorption capacity at atmospheric pressure and high temperature. Tea twigs can be used as raw material for activated carbon due to a high carbon content (53%). This research was conducted to produce activated carbon through carbonization at 400°C for 1 hour using a flow of N_2, followed by physical activation using Arc Plasma, which can generate high heat in a short time compared to electric furnace. Activation temperature variations from 600-800°C were applied in this study to observe their effects on the characteristics of the produced activated carbon. Characterization analysis including surface area, functional group formation, as well as crystal structure and size, were conducted using Brunauer-Emmett-Teller (BET), Fourier transform infrared (FTIR), and X-ray diffraction (XRD) analyses, respectively. Morphological changes in the activated carbon from plasma activation were presented through Scanning Electron Microscope (SEM) analysis. The performance of the activated carbon in adsorbing CO_2 was measured using Temperature-Programmed Desorption of CO_2 ($TPD\text{-}CO_2$) at a temperature of 40°C and a pressure of 1 atm. The optimum surface area obtained in this study was 86.668 $m^2\ g^{-1}$ with an adsorption capacity of 2.057 mmol g^{-1}, which was achieved at a physical activation temperature of 700°C with an activation time of 4 minutes using Arc Plasma.

Keywords: Activated Carbon; Adsorption; Arc Plasma; Carbon Dioxide; Tea Twigs.

1. Introduction

According to data from the International Energy Agency (Agency, 2023), CO_2 concentrations in the atmosphere are increasing by 1% each year. This condition has several impacts on the environment, including climate change and rising surface temperatures. The burning of fossil fuels in various industries, such as power generation, contributes to CO_2 emissions in the atmosphere. Therefore, efforts are needed to reduce the amount of CO_2 emissions through various mitigation measures, including separating CO_2 from industrial waste gases using CO_2 separation methods.

Current technologies for separating CO_2 from waste gases include absorption, adsorption, membranes, and cryogenic distillation. Among these technologies, adsorption has gained considerable attention and can serve as an alternative strategy for CO_2 separation from waste gases. The advantages of the adsorption process include high absorption capacity, good selectivity, efficient regeneration, favorable adsorption and desorption kinetics, excellent chemical stability, and low energy consumption (Gomez-Delgado *et al*., 2022; Guo *et al*., 2021; Gundogdu *et al*., 2012).

The CO_2 separation in this study focuses on the post-combustion waste gas condition, where the CO_2 concentration ranges from 3 until 20% (Lai *et al.*, 2021). Several types of solid adsorbents are used in the adsorption process, including zeolites, Metal Organic Frameworks (MOFs), and activated carbon. Among these solid adsorbents, activated carbon demonstrates superior CO_2 adsorption capacity at a pressure of 1 bar and a temperature of 40-60°C, which aligns with the operational conditions of post-combustion CO_2 (Lai and Ngu, 2024). Additionally, activated carbon exhibits hydrophobic properties and is insoluble in water, in contrast to zeolites, which are hydrophilic (Lai *et al.*, 2021; Devita Amelia, 2019).

Activated carbon can be produced from various materials with high carbon content. Other criteria needed for activated carbon production include low inorganic content, such as low ash content, minimal degradation during storage, and abundant availability in nature. Many studies have been conducted on activated carbon derived from biomass waste, including coconut shells (49.62%) (MN Mohd Iqbaldin, 2013), tea grounds (48,70%) (Zhou *et al.*, 2018), bagasse (Han *et al.*, 2019), palm kernel shell (51%) (Yek *et al.*, 2019), and rice husk (36.52%) (Boonpoke *et al.*, 2010).

Tea twigs were selected as the adsorbent material in this study due to their high carbon content (53.28%), low ash content (1.69%), volatile matter content of 76.59%, and high lignin content (39.5%). The high lignin content in the biomass can facilitate the formation of micropores in the biochar produced from carbonization (Eliasson and Carlsson, 2020; Kazemi Shariat Panahi *et al.*, 2020). In 2021, tea production in Indonesia reached 137,800 tons (Statistik, 2023). The amount of waste generated from tea processing in factories accounts for 3% of the total tea production, or 4,134 tons per year (Wulansari and Rezamela, 2020). The potential waste from tea twigs can account for up to 77% of the total tea waste (Rosyadi, 2018). Thus, the potential waste from tea twigs in Indonesia amounts to 3,183 tons per year.

The production of activated carbon involves two stages, namely carbonization and activation. Activation is divided into chemical activation and physical activation. Physical activation is an environmentally friendly method as it does not use chemicals. Generally, physical activation is performed at high temperatures of around 500-800°C with a slow heating rate, using steam, CO_2, or air. González *et. al.*, utilized activation temperatures of 750-800°C, yielding activated carbon with a surface area of 822-1,333 $m^2\ g^{-1}$ and a CO_2 adsorption capacity of 1.6-1.9 mmol g^{-1} (González-García *et al.*, 2013). However, activation temperatures above 850°C can lead to damage to porosity and a reduction in surface area. This indicates that activation temperature has a significant impact on the surface area and adsorption capacity of activated carbon.

Although physical activation is an environmentally-friendly activation method due to free from chemicals, it has a longer processing time, ranging from 1 to 8 hours (Heidarinejad *et al.*, 2020; Luo, 2020; Plaza-Recobert *et al.*, 2017; González-García *et al.*, 2013) . The use of thermal plasma in the production of activated carbon through microwave plasma has been studied by Kuptajit, *et. al.* (Kuptajit *et al.*, 2021). The results of the study demonstrated that heating with microwave plasma produces activated carbon with a surface area of 11-1,007 $m^2\ g^{-1}$ for 2 minutes. Therefore, the use of thermal plasma to produce activated carbon has potential for further research and development.

Arc Plasma is a device that generates thermal plasma through the ionization of gas between the potential difference of the anode and cathode with pulsed current. The Arc Plasma device does not have a temperature control, but it controls the electric current. In the Arc Plasma, there is a torch that serves as the site where electrical discharge occurs due to the potential difference between the cathode and anode. Argon gas is directed into the torch, which is equipped with a cooling water system. In addition to acting as a plasma-

forming gas, argon also provides protection to the material from oxidation. During the arc discharge, the cathode temperature is extremely high, and thermal electrons are emitted from the cathode. The light emitted from the plasma often contains lines originating from the cathode material. The heat generated by the Arc Plasma is controlled by adjusting the pulsed electric current, which acts as the input current source for heat generation. During operation, the temperature generated ranges between 600-2000℃, with a shorter heating time compared to electric furnace. The heat produced by the Arc Plasma can be measured using a thermocouple. The temperature readings on the thermocouple serve as the control parameter in the physical activation process. Arc Plasma Sintering has advantages of high energy density, low voltage, and high current. Currently, there is no application of Arc Plasma for activated carbon.

There has been no prior research on the synthesis of activated carbon through physical activation using Arc Plasma. Activation with Arc Plasma presents several benefits, including a shorter activation time compared to electric furnaces. In this study, we synthesized activated carbon through physical activation using Arc Plasma and then obtained the pore surface characteristics of the activated carbon through characterization tests. The resulting activated carbon from this study was used for CO_2 adsorption using Temperature-Programmed Desorption of CO_2 (TPD-CO_2) at a pressure of 1 bar and a temperature of 40°C. Brunauer-Emmett-Teller (BET) and Scanning Electron Microscope (SEM) characterization are also performed to determine the surface area of the activated carbon and to observe changes in the morphology or pore structure of the raw material and the produced activated carbon. To obtain information about the functional groups present in the activated carbon, as well as the structure and crystal size of the samples, Fourier transform infrared (FTIR) and X-ray diffraction (XRD) were conducted.

2. Methods

2.1. Raw Materials

Tea twigs that are not used in the tea production process were used as the main material in this study. The tea twigs were washed and rinsed with distilled water to remove impurities adhering to the raw material, ensuring that the raw material was clean. Excess moisture was removed by drying at 50°C for 3 days.

2.2. Experimental methods

2.2.1. Pretreatment

The raw material, tea twigs, undergoes pretreatment by drying in an oven at a temperature of 50-60°C until a moisture content of 10% is achieved. An electric grinder was used to crush the dried tea twigs into smaller particle sizes. Sieving was carried out manually to obtain a uniform quantity with a size between 170-200 mesh, which has been shown to be favourable for the physical synthesis of activated carbon.

2.2.2. Pyrolysis

A high-temperature furnace equipped with heating elements, a thermocouple, and a nitrogen gas flow system was used for the pyrolysis process. A total of 100 g of dried, crushed, and ground tea twigs were placed in the center of the furnace and heated to a pyrolysis temperature of 400°C, followed by the flow of inert nitrogen gas at a rate of 5 mL min^{-1} to maintain an inert atmosphere (Figure S1). Once the pyrolysis temperature was reached, the samples were held at the same temperature for 1 hour to determine the degree

of combustion or mass loss due to pyrolysis. The yield of pyrolyzed tea twigs (tea twigs char) was calculated as the mass ratio of the pyrolyzed sample to the input raw material. The biochar produced from the carbonization process is then filtered to obtain biochar with a particle size of 170-200 mesh.

Before the samples are physically activated in the Arc Plasma, the biochar needs to be compacted using a sample press. To compact the samples, poly(acrylic acid) $(C_3H_4O_2)_n$, Sigma Aldrich, CAS Number 9003-01-4, is used as a binder, along with distilled water as a solvent, and the filtered biochar. The ratio of biochar, binder, and distilled water is 1:0.1:0.5. The mixing of poly(acrylic acid) and distilled water is followed by heating on a hotplate at 50°C until a slurry is formed. The biochar is then mixed with the slurry and stirred thoroughly. The mixture is dried in an oven at 80°C for 5 hours. After that, the samples are pressed using a sample press. The pressure applied during pressing is 40 bar, with a holding time of 2 minutes.

2.2.3. Activation

The pressed samples undergo physical activation using Arc Plasma (see Figure 1). The samples are placed in a holder casing, and the sample holder motor is activated to bring the samples closer to the plasma torch. The parameters that influence physical activation are activation time and temperature. Each activated sample is treated for the same duration of 4 minutes. The choice of a 4 minute activation time is based on the optimal pore formation during the etching process influenced by thermal plasma, which can take up to 5 minutes (Lim *et al.*, 2023). Furthermore, the sample names for each variation are adjusted according to the temperature in the Arc Plasma during physical activation. The variations of activated carbon (AC) samples produced in this study include AC 600 (AC obtained from physical activation at 600°C), AC 700 (AC obtained from physical activation at 700°C), and AC 800 (AC obtained from physical activation at 800°C). The schematic of the activated carbon production process from tea twigs and physical activation with Arc Plasma can be seen in Figure S2.

2.3. Characterization

Evaluation of the physicochemical properties of the experimental samples was conducted through a series of characterization studies. Before any testing procedures were carried out, the samples were dried in an oven at 80°C for 4 hours to remove the adsorbed moisture. The activated samples were analyzed using SEM, BET, FTIR, and XRD characterizations. The morphology and topography of the samples were examined with SEM/EDS on a Hitachi SU-3500, Japan. Samples were prepared with gold coating at 18-25°C and observed at a magnification of X3000 under 10 kV conditions. Specific surface area determination and porosity analysis were conducted using a Micromeritics TriStar II 3020 instrument. The nitrogen adsorption/desorption isotherms were measured at 77 K (-196°C) in the relative pressure range of $0.05<P/P_0<1.00$ to characterize the textural parameters. The specific surface area (S_{BET}) and total pore volume (V_{TOT}) were calculated using the BET method at a relative pressure of 0.95. Prior to the experiments, the samples were outgassed under vacuum for 2 hours at 150°C to remove any adsorbed gases or moisture. All activated carbon samples were analyzed to identify the basic functional groups using Fourier Transform Infrared (FTIR) spectroscopy. The FTIR spectra were obtained using the standard Attenuated Total Reflection (ATR) method in the range of 4000 to 500 cm^{-1} (45 scans at a resolution of 2 cm^{-1}). The crystalline structure and degree of crystallinity of the activated carbons were examined using X-ray Diffraction (XRD) with a SmartLab Rigaku, equipped with CuKa radiation (λ=1.5418 Å) and a step size of 0.050 from 5 to 110°. The voltage supplied was 40 kV with a current of 30 mA.

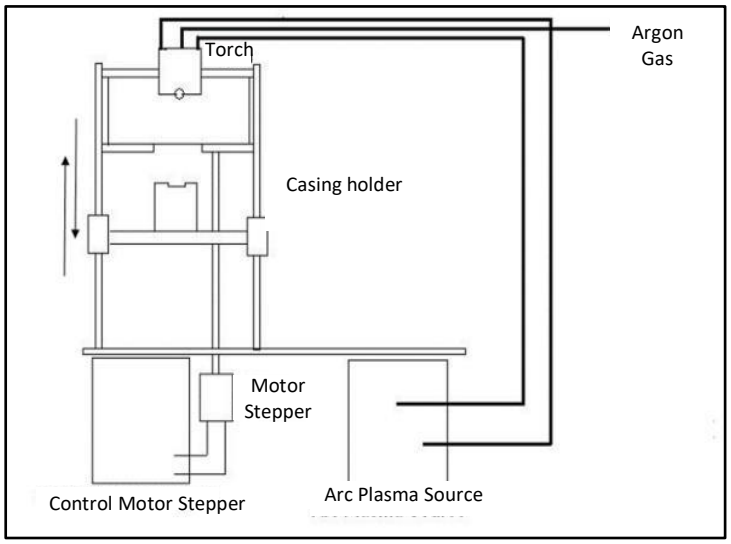

Figure 1 Scheme of Arc Plasma (scale 1:3)

The CO_2 adsorption test was conducted using Temperature-Programmed Desorption of CO_2 (TPD-CO_2) Micromeritics Autochem III (USA), involving several stages: pretreatment, adsorption, and desorption. The purpose of pretreatment is to remove volatile substances or impurities that remain on the surface of the activated carbon. The temperature and duration applied for pretreatment were 150°C and 60 minutes, respectively. Helium gas was flowed during the pretreatment process at a rate of 50 cm^3 min^{-1}. Previous research conducted by Klepel and Hunger investigated CO_2 adsorption through Temperature Programmed Desorption of CO_2 using a helium gas flow rate of 50 cm^3 min^{-1} (Klepel and Hunger, 2005). This flow rate was adopted for the gas flow rate in this study. A 55 mg of the sample was loaded into the reactor and heated from room temperature to 150°C at a heating rate of 30°C min^{-1} with a helium flow rate of 50 cm^3 min^{-1}, and the sample was treated at 150°C for 1 hour. Then, the CO_2 gas flow was maintained at 50 cm^3 min^{-1} for sample pre-saturation at 40°C held for 60 minutes. Subsequently, the sample was heated to 350°C at a heating rate of 10°C min^{-1} until the desorption equilibrium was reached.

3. Results and Discussion

3.1. Yield of Biochar and Activated Carbon

Carbonization is influenced by heating temperature, process duration, and the flow rate of inert gas. The temperature in the carbonization process plays a crucial role in the decomposition of organic compounds into pure carbon. Tabak *et. al.,* conducted thermal analysis (TGA) on tea twigs and identified three stages of decomposition: (1) at temperatures of 200-300°C, hemicellulose degradation occurs; (2) at 275-400°C, cellulose degradation takes place; and (3) at 250-500°C, lignin degradation occurs. To achieve a high carbon content in biochar, the degradation of hemicellulose, cellulose, and lignin is necessary, as this increases pore formation (Kazemi Shariat Panahi *et al.*, 2020, Meyer *et al.*, 2011). Therefore, a temperature of 400°C was chosen as the carbonization temperature in this study, maintained for 1 hour. Meanwhile, a temperature of 500°C is less optimal for carbonization as it may result in biochar with lower carbon content and yield. A temperature of 300°C was also not selected for carbonization, as the pore formation at this temperature was not yet optimal (Panwar *et al.*, 2019).

The yield of activated carbon is shown in Table S1. The carbonization process produces biochar with an approximate yield percentage of 35%. It has been reported that the expected yield from carbonizing biomass samples made from wood, under identical temperature and operational conditions, ranges from 34% to 49% (Mukherjee *et al*., 2022; Titiladunayo *et al*., 2012). This indicates that the research findings fall within the anticipated yield range. Nitrogen gas is flowed at a rate of 5 mL min^{-1} during the carbonization process to provide an inert atmosphere that prevents the biomass from undergoing oxidation. This is crucial to ensure that the carbon produced does not oxidize back into more volatile compounds or ash. The flow of nitrogen gas helps to remove volatile gases from the reactor, thereby enhancing the purity of the final carbon product. During the physical activation process, mass loss occurs due to the evaporation of residual water, the evaporation of volatile compounds, and the degradation of lignin. Lignin is completely degraded at temperatures between 160-900°C (Mahmoud and Ahmed, 2020; Tabak *et al*., 2019), therefore the mass loss during physical activation is also influenced by lignin degradation, which affects the yield values obtained.

Table S1 also presents the yield values from previous studies on activated carbon production. As indicated in Table S1, both activation temperature and time are crucial factors in determining the yield of activated carbon. In the study by Ogungbenro *et. al.,* (Ogungbenro *et al.*, 2018) activated carbon was produced from date seeds through a carbonization process followed by physical activation using CO_2 gas as the oxidizing agent (Table S1). The activation temperature in that study was varied between 600°C and 900°C, and it was found that as the temperature increased, the yield of activated carbon decreased. Ogungbenro *et. al.,* attributed this reduction in yield to the further decomposition of the lignocellulosic chemical components of the date seeds (Ogungbenro *et al.*, 2018). Their findings suggested that 800°C was the optimal activation temperature in a CO_2 atmosphere.

In the current study, physical activation was carried out using Arc Plasma, with Argon gas acting as the plasma source and also protecting the material from oxidation during the activation process. The yields achieved from activation temperatures ranging from 600°C to 800°C were between 83-90%, significantly higher than those obtained with CO_2 gas activation, as reported by Ogungbenro *et. al.,* (Ogungbenro *et al.*, 2018) (see Table S1). The use of Arc Plasma for physical activation resulted in higher yields compared to electric furnace. Additionally, the activation time played a critical role in determining the yield of the activated carbon.

In addition to the activation temperature, activation time also influences the yield capacity produced by the sample. The longer the sample is activated, the more the carbon content and volatile matter degrade and vaporize, while other minerals remain. Activation with Arc Plasma can be performed with a shorter activation time compared to electric furnace. The results of this study show that activation with Arc Plasma at 700°C for 4 minutes produces the highest yield (90%) compared to previous studies.

Arc Plasma activation offers the advantage of higher yield values due to the shorter activation time and the ability to generate heat more quickly compared to electric furnace. The decrease in carbon content during activation not only affects the yield of activated carbon but also the adsorption capacity of the resulting activated carbon. Additionally, the polar nature of activated carbon, which arises from the reactivity of surface functional groups formed by elemental deposits from the precursor, plays an important role in the adsorption performance of the produced activated carbon. The presence of functional groups in tea twigs and the resulting activated carbon can be investigated using FTIR techniques and will be discussed in the following section.

Other studies presented in Table S1 show high activated carbon yield values, ranging from 71-78%. The role of chemical activation agents is crucial in achieving high yield values, as reported in previous studies where the yield of activated carbon from chemical activation processes was around 35-78% (Table S1). The high yield values from chemical activation processes are likely due to treatments applied during activated carbon production. Studies that report high activated carbon yields typically involve mixing the raw materials with activation agents before proceeding with carbonization at temperatures of 600-900°C for 1-2 hours. The treatment with activation agents during the activated carbon production process affects the yield values produced. However, few studies report activated carbon production through carbonization followed by physical activation using CO_2 or steam, followed by nitrogen gas flow. This study demonstrates activated carbon production through carbonization followed by physical activation using Arc Plasma with an inert Argon gas flow to generate plasma and protect the material from oxidation during the activation process. The yield values obtained in this study are higher compared to previous studies that used a furnace with CO_2 gas flow for physical activation, and the yield values in this study are also higher than those obtained from activated carbon using chemical activation agents. This indicates that activated carbon production with Arc Plasma results in lower carbon and volatile matter loss, leading to higher yields.

3.2. Spectroscopic Analysis

The CO_2 adsorption capacity of activated carbon can be observed through its functional groups. Fourier transform infrared (FTIR) transmission spectra was conducted to obtain the wavenumber values indicating the presence of functional groups of the tea twigs and activated carbon samples. The tea twigs that have not undergone pyrolysis or activation exhibit more absorption bands than the activated carbon samples. This is indicative of the lignocellulosic nature of the tea twigs and the presence of various functional groups such as alkenes, esters, aromatics, alkanones, alcohols, hydroxyl groups, ethers, and carboxyl groups (Putri *et al.*, 2025). The IR absorption band at 3654 cm^{-1} signifies the presence of hydroxyl groups (OeH stretching between 3601 and 3317 cm^{-1}) in the tea twigs.

Functional groups that can enhance CO_2 adsorption include hydroxyl groups (O-H) with wavenumbers between 3200-3700 cm^{-1}, aromatic groups (C=C) with wavenumbers ranging from 1566-1650 cm^{-1}, and C-O groups with wavenumbers between 1050-1310 cm^{-1}. FTIR results indicate that all samples subjected to physical activation at AC 600, AC 700, and AC 800 contains hydroxyl (O-H) groups (see Figure 2). The role of hydroxyl (O-H) groups in CO_2 adsorption is to form hydrogen bonds with CO_2 molecules. These hydrogen bonds enhance the interaction between the surface of the activated carbon and CO_2 molecules. AC 800 shows a higher number of wave numbers and greater wave number values for hydroxyl (O-H) groups compared to the samples activated at 600^0C and 700^0C.

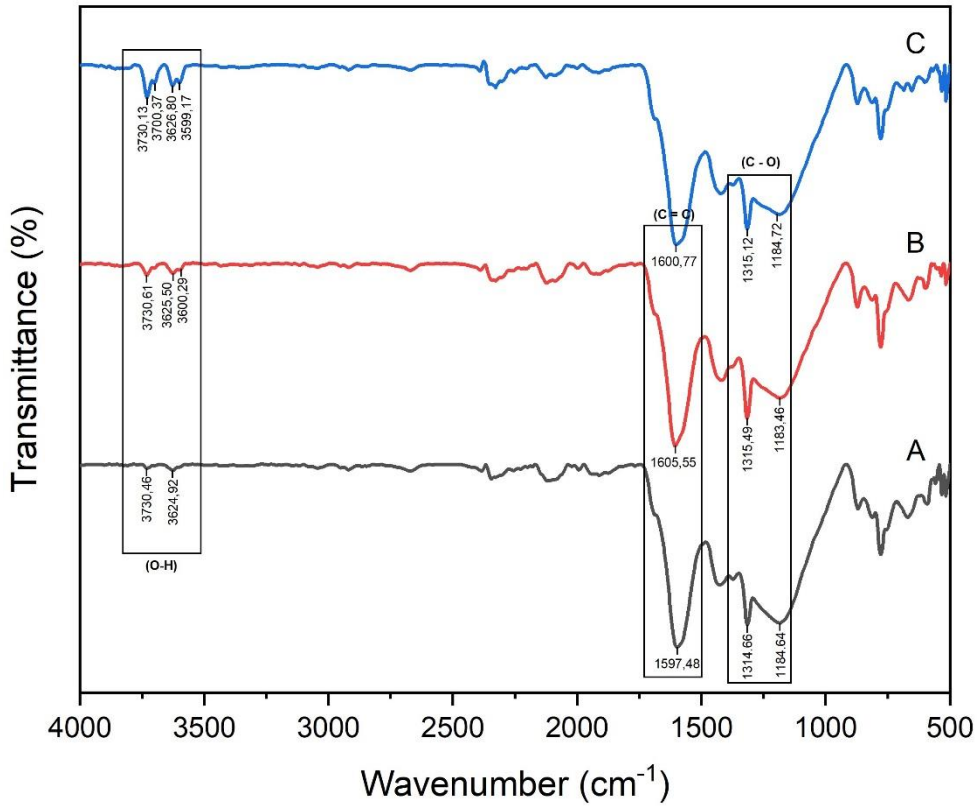

Figure 2 Functional groups of arc plasma activated carbon at (A) 600°C, (B) 700°C, and (C) 800°C

In addition, each sample contains aromatic (C=C) functional groups, which possess electrophilic properties beneficial for CO_2 adsorption. This is because CO_2 acts as a nucleophile and reacts with the electrophilic sites on the aromatic ring. Furthermore, each sample has C-O functional groups that can impart a negative charge to the carbon surface, enhancing electrostatic interactions and bonding with CO_2 molecules. The AC 800 shows a significant wave number for the C-O functional group. Each sample demonstrates the ability to adsorb CO_2 based on its functional group content.

3.3. Pattern of Diffraction Analysis

The diffraction patterns from the X-ray diffraction (XRD) analysis for samples are shown in Figure 3. For reference, the XRD diffraction pattern of activated carbon typically displays two diffraction peaks at 2-theta = 24-25° and 43° (Fahmi Puteri *et al.*, 2021; Omri and Benzina, 2012). The samples treated with the Arc Plasma at 600^{0}C, 700^{0}C, and 800^{0}C exhibit a diffraction peak at 2-theta = 24°, indicating that the samples align well with the XRD diffraction pattern of activated carbon. Additionally, the XRD patterns for each sample tend to show relatively broad and not very sharp peaks, suggesting that the samples possess an amorphous carbon structure. A weak peak is observed at 2-theta = 43°, which is likely caused by diffraction from the amorphous structure, indicating that physical activation leads to a decrease in the random structure (Borah *et al.*, 2015).

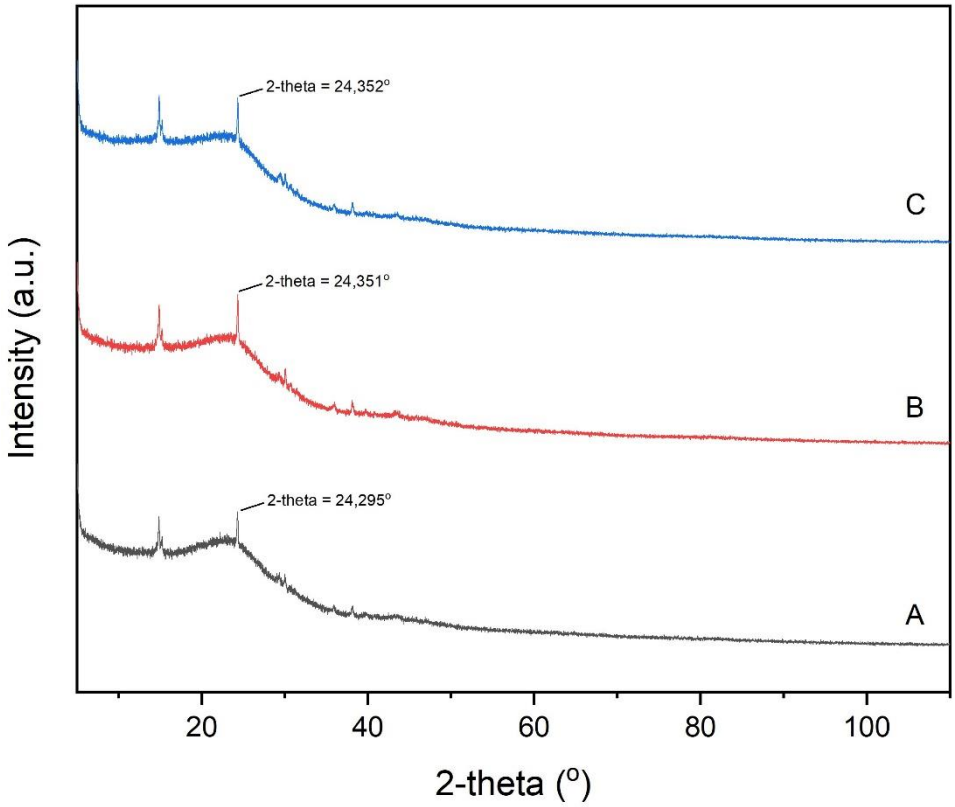

Figure 3 Diffraction Patterns of arc plasma activated carbon at (A) 600°C, (B) 700°C, and (C) 800°C

Table S2 presents a comparison of the FWHM values and crystal sizes at the peak of 2-theta = 24°. It can be seen that the carbon activated at relatively higher temperatures around 800°C yields smaller crystal size values compared to the carbon activated at 600°C and 700°C.The crystal size value of the obtained activated carbon sample is approximately 0.36 nm. This value is larger than that of graphite (0.335 nm). The increase in temperature during physical activation indicates a widening of the peak and a decrease in crystal size, which corresponds to an increase in porosity and a more amorphous structure (Chatterjee *et al*., 2020). The sample activated at 800^0C has the largest FWHM and the smallest crystal size, indicating the highest porosity among the three samples. This phenomenon is consistent with the literature on carbon produced from corncob (Sun and Webley, 2010). The increase in the surface area of activated carbon leads to a decrease in the crystal size value, which is caused by the densification of the material's structure (Jjagwe *et al.*, 2021). These XRD results align with the BET characterization results, showing that the activated carbon sample at 800^0C has a larger surface area compared to those activated at 600^0C and 700^0C.

3.4. Morphology Analysis

Scanning Electron Microscope (SEM) characterization was used to obtain morphological and topographical images of the tea twigs and produced activated carbons. Figure S3 (a) depicts the surface of the raw material, which remains non-porous due to the absence of thermal treatment. Biomass raw materials contain cellulose and lignin, which influence the characteristics of pore surfaces and the surface area of activated carbon. During the carbonization process, thermal decomposition takes place, in which lignin and

cellulose undergo a series of reactions that transform these organic substances into carbon, resulting in biochar. The elemental pores observed in the biochar sample are formed from the removal of most non-carbon elements during carbonization, resulting in a monolithic carbon framework. The thermal decomposition of biomass during carbonization also generates tar, which clogs the pores. As shown in Figure S3 (b), the pores formed are still obstructed by tar due to the thermal breakdown of biomass. The extensive tar formation during carbonization leads to biochar from tea twigs having a low specific surface area. As the biomass decomposes and volatile compounds are released during carbonization, the carbon content of the material increases while oxygen and hydrogen content decreases. This results in biochar being richer in carbon, making it a promising material for use as an adsorbent.

Figure S4 shows the well-formed and distinct pores in activated carbon. As the activation temperature increases from 600°C to 700°C and then to 800°C, the porosity development becomes more evident (Figure S4 (a-c)). The figure demonstrates the gradual formation of pores as the activation temperature rises. At lower temperatures, pore formation is partial, but as the temperature increases, broader micropores begin to develop. Moreover, pore creation in activated carbon can also be attributed to etching caused by the free electrons generated during the process. Higher electric current settings during Arc Plasma activation lead to more electrons being produced and greater heat generation. As heat increases, selective etching occurs, which optimizes the removal of volatile impurities and eliminates hydrocarbon contaminants from the biochar, thus expanding the cavity structure. Arc Plasma activation enhances the pore structure of the activated carbon, and larger, well-formed pores are clearly visible on the surface of the AC 800 sample (Figure S4 (c)). Higher activation temperatures lead to pore collapse. These well-developed pores are essential for improving the CO_2 adsorption capacity of activated carbon.

3.5. Porosity and Surface Area Analysis

The characteristics of the pore surface in activated carbon can be determined through analysis using the Brunauer-Emmett-Teller (BET) method. The BET results for the activated carbon samples indicate that the largest pore surface area was obtained from AC 800 (Table 1).

Table 1 Results of BET Characterization

No	Samples	S_{BET} ($m^2 g^{-1}$)	V_{total} ($cm^3 g^{-1}$)	V_{micro} ($cm^3 g^{-1}$)	V_{meso} ($cm^3 g^{-1}$)	D (nm)
1	Biochar	13.920	0.041	0.040	0.001	12.340
2	AC 600	80.189	0.115	0.096	0.019	2.737
3	AC 700	84.876	0.138	0.072	0.066	2.340
4	AC 800	86.668	0.157	0.039	0.118	2.118

S_{BET} = Specific surface area calculated with the BET method
V_{tota} = Total pore volume calculated at $P/P_0 = 0.99$
D = Pore size (nm)
V_{micro} = Micropore volume calculated by t-plot method
V_{meso} = Mesopore volume calculated from $V_{total} - V_{micro}$

Table 1 illustrates the increase in surface area and pore volume of biochar produced through carbonization and biochar activated with Arc Plasma at temperatures of 600°C, 700°C, and 800°C. The biochar obtained from carbonization has a surface area of 13.920 $m^2 g^{-1}$. The properties of the adsorbent raw materials, including the volatile matter content in biomass precursors, have a significant impact on porosity development, although they do

not influence the adsorption properties due to the creation of inert sites within the pores of the activated carbon (Putri *et al.*, 2025). The presence of volatile matter in the raw material can be eliminated during the carbonization process, as the tea twigs undergo thermal decomposition, leading to the formation of tar that blocks the pores and reduces the surface area (Karume *et al*., 2023). In the study reported by Putri et al., the raw material of tea twigs has a high volatile matter content of 76.59% (Putri *et al*., 2025). However, volatile matter can be eliminated during the carbonization process, as during carbonization, the tea twigs undergo thermal decomposition. Biochar from tea twigs has a low surface area due to the relatively high formation of tar during carbonization, which is a result of thermal decomposition to remove the relatively high volatile matter content in the tea twigs. Thus, the formation of relatively high tar during carbonization results in the blocking of pores, leading to a low surface area of the biochar.

Tea twigs have a low non-volatile content and a flammable physical structure, both of which contribute to a low ash content of 1.69% (Putri *et al.*, 2025). Precursor with a low ash content typically produce activated carbon with improved porosity, as there are fewer inert materials that hinder pore formation during the activation process. The reduced ash content allows a greater amount of carbon to contribute to pore formation, leading to an effective pore size suitable for adsorption. The results of the study indicate that activated carbon samples from Arc Plasma activation exhibit pore sizes ranging from 2.1 to 2.7 nm, which are similar to those of micropores. The relatively low specific surface area, despite the pore size being close to that of micropores, is likely due to incomplete pore formation during the Arc Plasma activation. Activation time plays a critical role in pore development, as noted in the study by Ogungbenro *et. al.*, (Ogungbenro *et al.*, 2018). As the activation time increases, more carbon content and volatile matter are degraded and vaporized. Short activation times with Arc Plasma lead to incomplete pore formation, making the activation process less effective, even though the resulting samples have pore sizes similar to those of micropores. However, shorter activation times result in higher yields. Therefore, in this study, an activation time of 4 minutes was chosen to achieve optimal micropore development, as the etching process influenced by thermal plasma takes up to 5 minutes (Lim *et al.*, 2023).

The physical or thermal activation treatment using Arc Plasma results in increased surface area and pore volume, as well as changes in pore size on the surface of activated carbon. This indicates that activation with Arc Plasma causes a greater increase in porosity within the sample's surface structure. As the activation process begins, pore development occurs gradually. At low combustion temperatures, pore development occurs partially, and as the combustion temperature increases, wider micropore development takes place, as indicated by the larger surface area and pore volume (see Table 1).

Utilizing Arc Plasma for physical or thermal activation in the production of activated carbon is an innovation, as improvements in surface area have traditionally been achieved through chemical activation using basic or acidic activating agents such as KOH, NaOH, $ZnCl_2$, or H_3PO_4. There is currently no literature that describes the mechanism of pore formation using Arc Plasma; however, fundamentally, Arc Plasma is a type of thermal plasma generated through gas ionization. Argon gas is used as an inert gas in the activation of biochar with Arc Plasma. When ionization occurs between Argon (Ar) inert gas under the potential difference between the anode and cathode with pulsed current, electrons are released from Argon atoms, generating positive Argon ions (Ar^+) and free electrons (e^-). Carbon is a conductive material that has electrons moving within its structure. When the carbon material is exposed to electrons, the free electrons in the carbon respond by moving, creating eddy currents. These currents flow in a closed circular pattern within the

conductor, causing resistance and the release of heat. When the size of the biochar is larger than the depth of the skin effect of the generated current, the surface of the biochar can be locally heated. This thermal effect leads to pore formation on the biochar surface, resulting in a porous activated carbon material. Additionally, pore formation in activated carbon can occur due to the etching caused by the free electrons generated. The higher the electric current setting, the more electrons are generated and the greater the heat produced. This study applied variations of temperatures of 600°C, 700°C, and 800°C, for physical activation. The increase in activation temperature positively affects the increase in surface area. Activated carbon treated with Arc Plasma at temperature of 800^0C achieved a surface area of 86.668 m^2 g^{-1}, a pore volume of 0.157 cm^3 g^{-1}, and a pore size of 2.118 nm. This surface area value is larger than that of the other samples. The increase in activation temperature can optimize the removal of volatile impurities and eliminate hydrocarbon contaminants from the biochar produced during carbonization, as well as enlarge the cavity structure, thereby increasing the surface area (Ramadhani *et.al.,* 2020; Yuliusman *et. al.,* 2015).

Based on pore size and volume, the pores in the biochar produced from carbonization are classified as mesopores, with a pore size of 12.340 nm and a pore volume of 0.041 cm^3 g^{-1}. In contrast, the activated carbon samples subjected to physical activation are classified as micropores, with pore sizes ranging from 2.118 to 2.727 nm and pore volumes of 0.115 to 0.157 cm^3 g^{-1} (Phothong *et al.*, 2021). The physically activated carbon samples exhibit a greater CO_2 adsorption capacity compared to the biochar samples, due to their smaller pore sizes. Pore sizes of 1-2.5 nm are optimal for gas adsorption, particularly for CO_2 (Chen *et al.*, 2017). This will be discussed further in the following section.

3.6. CO_2 Adsorption Studies

The CO_2 adsorption capacity was conducted using a Temperature Programmed Desorption of CO_2 (TPD-CO_2). The adsorption capacity data for each sample, including those obtained from carbonization and the activated carbon samples treated with Arc Plasma at activation temperature of 600^0C, 700^0C, and 800^0C, can be seen in Table 2.

Table 2 Adsorption of CO_2 from Biochar, AC 600, AC 700, and AC 800 (in mmol g^{-1})

No	Samples	Specific Surface Area (m^2 g^{-1})	Pore Volume (cm^3 g^{-1})	Pore Size (nm)	CO_2 Adsorption (mmol/g)
1	Biochar	13.920	0.041	12.340	0.354
2	AC 600	80.189	0.115	2.737	1.816
3	AC 700	84.876	0.138	2.340	1.959
4	AC 800	86.668	0.157	2.118	2.057

The mechanism of the adsorption process can be explained in two ways: physical adsorption and chemical adsorption. Physical adsorption occurs due to factors such as surface area, pore volume, and pore size. Table 2 provides the physical characteristics of activated carbon that influence CO_2 adsorption capacity. The larger the surface area of activated carbon, the more active sites are available for the adsorption of CO_2 molecules. Data from Table 2 show a significant increase in surface area from biochar (13.920 m^2 g^{-1}) to physically activated carbon using Arc Plasma at temperature of 800^0C (86.668 m^2 g^{-1}). The growth in surface area is directly related to the improvement in CO_2 adsorption capacity, with biochar showing a capacity of 0.354 mmol g^{-1}, while the activated carbon

sample treated with Arc Plasma at 800°C reaches 2.057 mmol g^{-1}. This study demonstrates that activated carbon with a larger surface area can improve its ability to adsorb CO_2.

Figure S5 presents the graph showing the relationship between surface area (m^2 g^{-1}) and CO_2 adsorption capacity (mmol g^{-1}), indicating that a greater surface area leads to increased CO_2 adsorption. Additionally, a larger pore volume allows for more CO_2 molecules to be adsorbed into the structure of the activated carbon. Data in Table 4 reveal an increase in pore volume from 0.041 cm^3 g^{-1} in the biochar to 0.157 cm^3g^{-1} in the AC 800 sample. Increasing of pore volume contributes to the enhanced CO_2 adsorption capacity. A larger pore volume provides sufficient space for CO_2 molecules to enter and become trapped.

Figures S5 and S6 demonstrate that as the activation temperature increases, the CO_2 adsorption capacity also increases in a nearly linear manner. The increase in temperature accelerates the collision frequency of molecules, resulting in more effective reactions, or strengthens the Van der Waals forces, enabling CO_2 to diffuse more effectively into the reaction sites. This study's results also reveal a nearly linear correlation between CO_2 adsorption capacity and both specific surface area and pore volume, as shown in Figures S3 and S4. These findings align with previous reports that highlight the crucial role of specific surface area and pore volume in CO_2 absorption (Nurfarhana *et al.*, 2023, Salma Amaliani Putri, 2019). As the specific surface area of the adsorbent increases, a greater amount of adsorbate can be bound to the pores of the adsorbent (Mahmud Sudibandriyo, 2024, Salma Amaliani Putri, 2019).

Figure S6 shows the graph of the effect of pore volume on CO_2 adsorption capacity indicating that as pore volume increases, more CO_2 can be adsorbed. Activated carbon with mesopore sizes (around or larger than 30 Å or equivalent to 3 nm) is more suitable for liquid phase applications, while smaller pore sizes (10 to 25 Å or equivalent to 1 – 2.5 nm) are appropriate for gas phase applications, although the AC 600 sample, with a pore size of 2.737 nm, is still considered suitable for gas adsorption. Smaller pore sizes, which are closer to the size of CO_2 molecules, enhance the interaction between CO_2 molecules and the pore walls, thereby increasing adsorption capacity.

Table 3 Comparison of Research Results

No	Authors	Raw materials	Specific surface area (m^2 g^{-1})	CO_2 adsorption capacity (mmol/g)	Adsorption conditions (P, T)
1	(Rashidi *et al.*, 2014)	Commercial activated carbon	717.22	1.84	1 bar, 50^{0}C
2	(Kusrini *et.al.*, 2017)	Graphite waste	8.49 18.48 35.52	2.737 1.62 0.61	3 bar, 45^{0}C
3	(Joseph *et al.*, 2017)	Oil palm fruit bunch	14.32	1.93	1 bar, 25^{0}C
4	(Yıldız *et al.*, 2019)	Chicken manure waste	22.22	1.95	1 bar, 25^{0}C
5	(Ding and Liu, 2020)	Enteromorpha	60.2	0.52	1 bar, 25^{0}C
6	(Ding and Liu, 2020)	Sargassum	291.8	1.05	1 bar, 25^{0}C
4	AC 600 (in this study) AC 700 (in this study) AC 800 (in this study)	Tea twigs	80.189 84.876 86.668	1.816 1.959 2.057	1 bar, 40^{0}C

Table 3 presents a summary of the CO_2 adsorption capacity of the activated carbon samples, comparing the data with existing literature. The activated carbon sample with the highest CO_2 adsorption capacity in this study is 2.057 mmol g^{-1}, which is consistent with the CO_2 adsorption capacity of commercial activated carbon (Table 3). Moreover, Table 3 includes literature results showing that although activated carbon with smaller surface areas was used, its CO_2 adsorption capacity is still comparable to that of commercial activated carbon. In addition to the specific surface area, the pore size of the material also plays a role in influencing CO_2 adsorption capacity. Smaller pores generally exhibit higher CO_2 adsorption, and as the pore size increases, the CO_2 adsorption capacity tends to decrease (as seen in Table 2). These results are in agreement with previous studies (Chen *et al.*, 2017). The pore size of the activated carbon samples derived from Arc Plasma activation falls between 2.1-2.7 nm, which is near the micropore size range. Most CO_2 adsorption in activated carbon occurs within micropores (pores smaller than 2 nm in diameter). Smaller pores enable more CO_2 molecules to be adsorbed, as CO_2 molecules are more effectively trapped within the activated carbon, thus reducing the chances of gas escaping before complete absorption. Smaller pores can also reduce the CO_2 diffusion rate, enhancing the efficiency of adsorption and maximizing adsorption capacity.

Figure 6 shows the interaction between CO_2 gas molecules and the adsorbent surface, as well as the energy needed to release CO_2 from the surface. The curve presents peaks that indicate the temperature at which CO_2 starts to desorb from the surface. A higher peak suggests a stronger bond between CO_2 and the adsorbent surface, necessitating a higher temperature for desorption. In contrast, a lower peak represents a weaker bond, enabling CO_2 to be released at a lower temperature. The peak at a lower temperature signifies physisorption, where CO_2 is held by weaker Van der Waals forces on the adsorbent surface. The peak at a higher temperature point to chemisorption, where CO_2 is more strongly attached through chemical bonds, requiring a higher temperature for desorption.

The curves of samples AC 600, AC 700, and AC 800 show two distinct peaks, which suggest the existence of homogeneous active sites. The curve with a higher sharp peak indicates that a significant amount of energy is needed for CO_2 desorption, while the one with a lower sharp peak requires less energy for desorption. These sharp peaks are evident across all samples, with the first peak corresponding to CO_2 release at a lower temperature (<200°C), suggesting minimal energy required and indicating physisorption. In contrast, the second peak, which is broader, signifies the presence of heterogeneous active sites. This second peak reflects a chemisorption phenomenon, where CO_2 is strongly bonded and needs a higher temperature (>200°C) to be desorbed. All samples exhibit a more pronounced chemisorption behaviour during CO_2 adsorption, likely influenced by the adsorption temperature used.

CO_2 lacks a dipole but has a significant quadrupole moment. Its linear shape and polar bonds at both ends enable it to interact easily with active sites on the surface of the char (Goel *et al.*, 2021). At lower adsorption temperatures, CO_2 molecules have reduced kinetic energy, making them more likely to be adsorbed and held on the surface of the adsorbent. As a result, low temperatures are generally used to improve CO_2 adsorption capacity, as demonstrated in Table 6. While many studies examine adsorption at room temperature, fewer provide data on CO_2 adsorption capacities at temperatures higher than room temperature. The findings of this study indicate that a relatively high CO_2 adsorption capacity is achieved at an adsorption temperature of 40°C. However, adsorption at temperatures slightly above room temperature is mainly governed by chemisorption mechanisms, as shown in Figure 6.

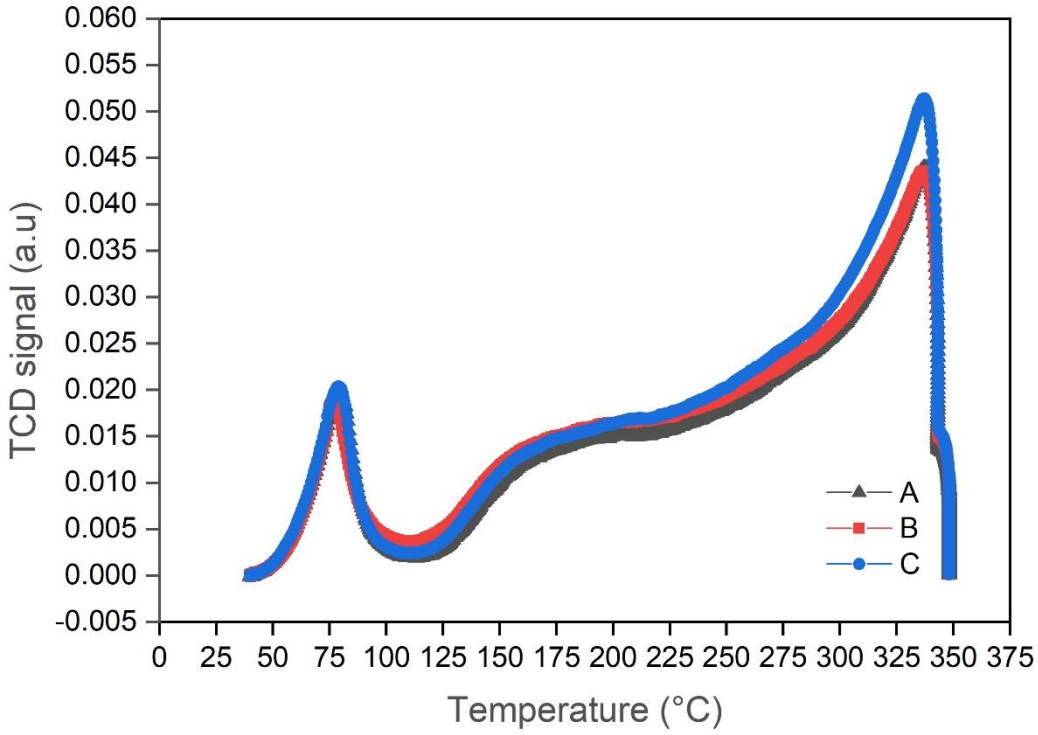

Figure 6 Temperature Programmed Desorption of CO_2 (TPD-CO_2) curve of arc plasma activated carbon at (A) 600°C, (B) 700°C, and (C) 800°C

At 40°C, adsorption starts due to the attractive forces between CO_2 molecules and the activated carbon surface. However, the Van der Waals forces at play are relatively weak, which is reflected in the first peak being both low and sharp. As the temperature increases during adsorption, the interaction between CO_2 molecules and the atoms or ions on the activated carbon surface strengthens, leading to the formation of chemical bonds and heterogeneous active sites. A high desorption temperature is needed to break these chemical bonds, as indicated by the higher and broader second peak. The chemisorption effect is more pronounced in all samples, as the area under the second peak is larger than that under the first peak. All samples exhibit weak Van der Waals interactions, but as the temperature rises during adsorption, stronger chemical bonds are formed between CO_2 molecules and the activated carbon surface. This suggests that the adsorption temperature plays a crucial role in determining the adsorption mechanism.

The findings of this study are in agreement with earlier research on CO_2 adsorption performance, which demonstrated that CO_2 adsorption at lower temperatures enhances the efficiency of physical adsorption. Physisorption is more effective at lower adsorption temperatures as it facilitates better trapping of CO_2 molecules within the smaller pores of activated carbon. Additionally, lower temperatures help preserve the stability and adsorption capacity of activated carbon, which is essential for effective CO_2 adsorption (Zubbri *et al.*, 2021, Huang *et al.*, 2019).

4. Conclusions

This study investigates the production of activated carbon from tea branch biomass through a carbonization process followed by physical activation using Arc Plasma. The resulting activated carbon was analysed to assess its pore characteristics, and CO_2

adsorption tests were conducted. The properties examined include surface area, morphological structure, presence of functional groups, and the crystallinity of the activated carbon pores. This research on activated carbon with Arc Plasma activation is a novel approach, and the findings demonstrate that the CO_2 adsorption capacity of the activated carbon derived from tea branch biomass through Arc Plasma activation is 2.057 mmol g^{-1}. Arc Plasma presents advantages by reducing the activation time and yielding activated carbon with a high adsorption capacity. In conclusion, the activated carbon adsorbent from tea branches, activated with Arc Plasma, shows great potential for CO_2 adsorption applications, offering a short activation time. Further investigations are needed to explore the selectivity of CO_2 separation from gas streams and the material's performance under various adsorption conditions, which will be the focus of future research.

Acknowledgments

The authors acknowledge the facilities, scientific and technical support from Advanced Characterization Laboratories Serpong, National Research and Innovation Institute through E-Layanan Sains, Badan Riset dan Inovasi Nasional. The authors disclosed receipt of the following financial support for the research, authorship, and/or publication of this article: This research was funded and supported by Doctoral's program scholarship of the Indonesian education scholarship, Lembaga Pengelola Dana Pendidikan (LPDP). The research was also supported by the program of Hibah Pendanaan Penelitian Kemendikbudristek Tahun 2024, grant numbers 051/E5/PG.02.00.PL/2024 and 350/PKS/WR III/UI/2024, which was granted by the Kementerian Pendidikan, Kebudayaan, Riset dan Teknologi (Kemendikbudristek) in 2024.

Conflict of Interest

The authors declare no conflicts of interest.

References

Badan Pusat Statistik (BPS), 2023. Indonesia Tea Statistics, Badan Pusat Statistik, Jakarta, Indonesia

Boonpoke, A., Chiarakorn, S., Laosiripojana, N., Towprayoon, S., Chidthaisong, A., 2010. Synthesis Of Activated Carbon And MCM-41 From Bagasse And Rice Husk And Their Carbon Dioxide Adsorption Capacity. *Journal of Sustainable Energy & Environment*, Volume 2, pp. 77-81. https://api.semanticscholar.org/CorpusID:53580943

Borah, L., Goswami, M., Phukan, P., 2015. Adsorption Of Methylene Blue And Eosin Yellow Using Porous Carbon Prepared From Tea Waste: Adsorption Equilibrium, Kinetics And Thermodynamics Study. *Journal Of Environmental Chemical Engineering,* Volume 3**,** pp. 1018-1028. https://doi.org/10.1016/j.jece.2015.02.013

Chatterjee, R., Sajjadi, B., Chen, W.-Y., Mattern, D. L., Hammer, N., Raman, V., Dorris, A., 2020. Effect of Pyrolysis Temperature on PhysicoChemical Properties and Acoustic-Based Amination of Biochar for Efficient CO_2 Adsorption. *Frontiers in Energy Research,* Volume 8, https://doi.org/10.3389/fenrg.2020.00085

Chen, L., Watanabe, T., Kanoh, H., Hata, K., Ohba, T., 2017. Cooperative CO_2 Adsorption Promotes High CO_2 Adsorption Density Over Wide Optimal Nanopore Range. *Adsorption Science & Technology,* Volume 36**,** pp. 625-639. https://doi.org/10.1177/0263617417713573

Ding, S., Liu, Y., 2020. Adsorption of CO_2 From Flue Gas By Novel Seaweed-Based KOH-Activated Porous Biochars. *Fuel,* Volume 260**,** pp. 116382. https://doi.org/10.1016/j.fuel.2019.116382

Eliasson, J., Carlsson, V., 2020. *Agricultural Waste And Wood Waste For Pyrolysis And Biochar : An Assessment For Rwanda.* Independent Thesis Basic Level (Degree Of Bachelor) Student Thesis.

Fahmi Puteri, P., Cucun Alep, R., Yohanes, M., 2021. Karakterisasi Karbon Aktif Kulit Singkong (Manihot Esculenta Crantz) Berdasarkan Variasi Konsentrasi H_3PO_4 Dan Lama Waktu Aktivasi. *Indonesian Journal Of Chemical Analysis,* Volume 4**,** pp. 72-81. https://doi.org/10.20885/ijca.vol4.iss2.art4

Goel, C., Mohan, S., Dinesha, P., 2021. CO_2 Capture By Adsorption On Biomass-Derived Activated Char: A Review. *Science Of The Total Environment,* Volume 798**,** pp. 149296. https://doi.org/10.1016/j.scitotenv.2021.149296

Gomez-Delgado, E., Nunell, G., Cukierman, A. L., Bonelli, P.,, 2022. Agroindustrial Waste Conversion Into Ultramicroporous Activated Carbons For Greenhouse Gases Adsorption-Based Processes. *Bioresource Technology Reports,* Volume 18**,** pp. 101008. https://doi.org/10.1016/j.biteb.2022.101008

González-García, P., Centeno, T. A., Urones-Garrote, E., Ávila-Brande, D., Otero-Díaz, L. C., 2013. Microstructure And Surface Properties Of Lignocellulosic-Based Activated Carbons. *Applied Surface Science,* Volume 265**,** pp. 731-737. https://doi.org/10.1016/j.apsusc.2012.11.092

Gundogdu, A., Duran, C., Senturk, H. B., Soylak, M., Imamoglu, M., Onal, Y., 2013. Physicochemical Characteristics Of A Novel Activated Carbon Produced From Tea Industry Waste. *Journal Of Analytical And Applied Pyrolysis,* Volume 104**,** pp. 249-259. https://doi.org/10.1016/j.jaap.2013.07.008

Gundogdu, A., Duran, C., Senturk, H. B., Soylak, M., Ozdes, D., Serencam, H., Imamoglu, M., 2012. Adsorption Of Phenol From Aqueous Solution On A Low-Cost Activated Carbon Produced From Tea Industry Waste: Equilibrium, Kinetic, And Thermodynamic Study. *Journal Of Chemical & Engineering Data,* Volume 57**,** pp. 2733-2743. https://doi.org/10.1021/je300597u

Guo, Y., Sun, J., Wang, R., Li, W., Zhao, C., Li, C., Zhang, J., 2021. Recent Advances In Potassium-Based Adsorbents For CO_2 Capture And Separation: A Review. *Carbon Capture Science & Technology,* Volume 1**,** pp. 100011. https://doi.org/10.1016/j.ccst.2021.100011

Han, J., Zhang, L., Zhao, B., Qin, L., Wang, Y., Xing, F., 2019. The N-Doped Activated Carbon Derived From Sugarcane Bagasse For CO_2 Adsorption. *Industrial Crops And Products,* Volume 128**,** pp. 290-297. https://doi.org/10.1016/j.indcrop.2018.11.028

Heidarinejad, Z., Dehghani, M. H., Heidari, M., Javedan, G., Ali, I. & Sillanpää, M., 2020. Methods For Preparation And Activation Of Activated Carbon: A Review. *Environmental Chemistry Letters,* Volume 18**,** pp. 393-415. https://doi.org/10.1007/s10311-019-00955-0

Huang, G.-G., Liu, Y.-F., Wu, X.-X., Cai, J.-J., 2019. Activated Carbons Prepared By The KOH Activation Of A Hydrochar From Garlic Peel And Their CO_2 Adsorption Performance. *New Carbon Materials,* Volume 34**,** pp. 247-257. https://doi.org/10.1016/S1872-5805(19)60014-4

International Energy Agency (IEA), 2023. CO_2 Emissions In 2023. Paris.

Jjagwe, J., Olupot, P. W., Menya, E., Kalibbala, H. M., 2021. Synthesis And Application Of Granular Activated Carbon From Biomass Waste Materials For Water Treatment: A

Review. *Journal Of Bioresources And Bioproducts,* Volume 6, pp. 292-322. https://doi.org/10.1016/j.jobab.2021.03.003

Joseph, C. G., Quek, K. S., Daud, W. M. A. W., Moh, P. Y., 2017. Physical Activation Of Oil Palm Empty Fruit Bunch Via CO_2 Activation Gas For CO_2 Adsorption. *In: IOP Conference Series: Materials Science And Engineering,* Volume 206**,** pp. 012003. https://doi.org/10.1088/1757-899X/206/1/012003

Karamah, E.F., Anindita, L., Amelia, D., Kusrini, E., Bismo, S., 2019. Tofu Industrial Wastewater Treatment with Ozonation and the Adsorption Method using Natural Zeolite . *International Journal of Technology*. Volume 10(8), pp. 1498-1504. https://doi.org/10.14716/ijtech.v10i8.3471

Karume, I., Bbumba, S., Tewolde, S., Mukasa, I. H. Z. T., Ntale, M., 2023. Impact Of Carbonization Conditions And Adsorbate Nature On The Performance Of Activated Carbon In Water Treatment. *BMC Chemistry,* Volume 17**,** pp. 162. https://doi.org/10.1186/s13065-023-01091-1

Kazemi Shariat Panahi, H., Dehhaghi, M., Ok, Y. S., Nizami, A.-S., Khoshnevisan, B., Mussatto, S. I., Aghbashlo, M., Tabatabaei, M., Lam, S. S., 2020. A Comprehensive Review Of Engineered Biochar: Production, Characteristics, And Environmental Applications. *Journal Of Cleaner Production,* Volume 270**,** pp. 122462. https://doi.org/10.1016/j.jclepro.2020.122462

Klepel, O. & Hunger, B., 2005. Temperature-Programmed Desorption (TPD) Of Carbon Dioxide On Alkali-Metal Cation-Exchanged Faujasite Type Zeolites. *Journal Of Thermal Analysis And Calorimetry,* Volume 80**,** pp. 201-206. https://doi.org/10.1007/s10973-005-0636-3

Kuptajit, P., Sano, N., Nakagawa, K., Suzuki, T., 2021. A Study On Pore Formation Of High Surface Area Activated Carbon Prepared By Microwave-Induced Plasma With KOH (Miwp-KOH) Activation: Effect Of Temperature-Elevation Rate. *Chemical Engineering And Processing - Process Intensification,* Volume 167**,** pp. 108511. https://doi.org/10.1016/j.cep.2021.108511

Kusrini, E., Sasongko, A.K., Nasruddin., Usman, A., 2017. Improvement of Carbon Dioxide Capture using Graphite Waste/ FE_3O_4 Composites. *International Journal of Technology*. Volume 8(8), pp.1436-1444. https://doi.org/10.14716/ijtech.v8i8.697

Lai, J. Y., Ngu, L. H., 2024. Post-Combustion Carbon Dioxide Adsorption Of Concurrent Activated And Surface Modified Palm Kernel Shell-Derived Activated Carbon. *Greenhouse Gases: Science And Technology,* Volume 14**,** pp. 492-525. 10.1002/ghg.2274

Lai, J. Y., Ngu, L. H., Hashim, S. S., 2021. A Review Of CO_2 Adsorbents Performance For Different Carbon Capture Technology Processes Conditions. *Greenhouse Gases: Science And Technology,* Volume 11**,** pp. 1076-1117. https://doi.org/10.1002/ghg.2112

Lim, C., Kwak, C. H., Jeong, S. G., Kim, D., Lee, Y.-S., 2023. Enhanced CO_2 Adsorption Of Activated Carbon With Simultaneous Surface Etching And Functionalization By Nitrogen Plasma Treatment. *Carbon Letters,* Volume 33**,** pp. 139-145. https://doi.org/10.1007/s42823-022-00410-1

Luo, Y., Wang, K., And Fei, L., 2020. The Effects Of Activation Conditions On Physical Properties Of Activated Carbon. *Bioresources,* Volume 15**,** pp. 7640-7647. https://doi.org/10.15376/biores.15.4.7640-7647

Mahmoud, A., Ahmed, E., 2020. Biomass Carbonization. *In: Renewable Energy,* Mansour Al, Q., Ahmad, E.-K., Hakan Serhad, S. (ed.), Intechopen, Rijeka, London, England. https:// 10.5772/intechopen.90480

Malhotra, M., Suresh, S., Garg, A., 2018. Tea Waste Derived Activated Carbon For The Adsorption Of Sodium Diclofenac From Wastewater: Adsorbent Characteristics, Adsorption Isotherms, Kinetics, And Thermodynamics. *Environmental Science And Pollution Research,* Volume 25**,** pp. 32210-32220. https://doi.org/10.1007/s11356-018-3148-y

Meyer, S., Glaser, B., Quicker, P., 2011. Technical, Economical, And Climate-Related Aspects Of Biochar Production Technologies: A Literature Review. *Environmental Science & Technology,* Volume 45**,** pp. 9473-9483. https://doi.org/10.1021/es201792c

Iqbaldin, Mn Mohd., Khudzir, I., Azlan, MI Mohd., Zaidi, AG., Surani, B., Zubri, Z., 2013. Properties Of Coconut Shell Activated Carbon. *Journal Of Tropical Forest Science,* Volume 25, pp. 497-503. Retrieved from https://jtfs.frim.gov.my/jtfs/article/view/460

Mukherjee, A., Patra, B. R., Podder, J., Dalai, A. K., 2022. Synthesis Of Biochar From Lignocellulosic Biomass For Diverse Industrial Applications And Energy Harvesting: Effects Of Pyrolysis Conditions On The Physicochemical Properties Of Biochar. *Frontiers In Materials,* Volume 9. https://doi.org/10.3389/fmats.2022.870184

Nurfarhana, M. M., Asikin-Mijan, N., Yusoff, S. F. M., 2023. Porous Carbon From Natural Rubber For CO_2 Adsorption. *Materials Chemistry And Physics,* Volume 308**,** pp. 128196. https://doi.org/10.1016/j.matchemphys.2023.128196

Ogungbenro, A. E., Quang, D. V., Al-Ali, K. A., Vega, L. F., Abu-Zahra, M. R. M., 2018. Physical Synthesis And Characterization Of Activated Carbon From Date Seeds For CO_2 Capture. *Journal Of Environmental Chemical Engineering,* Volume 6**,** pp. 4245-4252. https://doi.org/10.1016/j.jece.2018.06.030

Omri, A., Benzina, M., 2012. Characterization Of Activated Carbon Prepared From A New Raw Lignocellulosic Material: Ziziphus Spina-Christi Seeds. *Journal De La Société Chimique De Tunisie,* Volume 14**,** pp. 175-183. http://www.sctunisie.org/pdf/JSCT_v14-22.pdf

Panwar, N. L., Pawar, A., Salvi, B. L., 2019. Comprehensive Review On Production And Utilization Of Biochar. *SN Applied Sciences,* Volume 1**,** pp. 168. https://doi.org/10.1007/s42452-019-0172-6

Phothong, K., Tangsathitkulchai, C., Lawtae, P., 2021. The Analysis Of Pore Development And Formation Of Surface Functional Groups In Bamboo-Based Activated Carbon During CO_2 Activation. *Molecules,* Volume 26**,** pp. 5641.

Plaza-Recobert, M., Trautwein, G., Pérez-Cadenas, M. & Alcañiz-Monge, J., 2017. Preparation Of Binderless Activated Carbon Monoliths From Cocoa Bean Husk. *Microporous And Mesoporous Materials,* Volume 243**,** pp. 28-38. https://doi.org/10.1016/j.micromeso.2017.02.015

Putri, A. M. H., Ramadhoni, B. F., Radias, M. S. H., Riyadi, F. A., Alam, M. Z., Muharam, Y., 2025. Performance Of Activated Carbon Derived From Tea Twigs For Carbon Dioxide Adsorption. *Current Research In Green And Sustainable Chemistry,* Volume 10, pp**.** 100440. https://doi.org/10.1016/j.crgsc.2024.100440

Ramadhani, L. F., Nurjannah, I.M., Yulistiani, R., Saputro, E.A., 2020. Review: Teknologi Aktivasi Fisika Pada Pembuatan Karbon Aktif Dari Limbah Tempurung Kelapa. *Jurnal Teknik Kimia*, Volume 26 (2), pp. 42-53. DOI: 10.36706/jtk.v26i2.518

Rashidi, N. A., Yusup, S., Borhan, A., Loong, L. H., 2014. Experimental And Modelling Studies Of Carbon Dioxide Adsorption By Porous Biomass Derived Activated Carbon. *Clean Technologies And Environmental Policy,* Volume 16**,** pp. 1353-1361. https://doi.org/10.1007/s10098-014-0788-6

Rosyadi, A.I., Harianto, S., Prawira-Atmaja, M.I., . S. S. H. M. D. D. R. A. I., 2018. Karakteristik Pelet Kayu Dari Limbah Pangkasan Teh Berdasarkan Besaran Partikel. *Jurnal Penelitian Teh Dan Kina,* Volume 21.

Sudibandriyo, M., Rizki, A., 2024. The Influence of Activated Carbon as Adsorbent in Adsorptive – Distillation of Ethanol–Water Mixture. *International Journal of Technology*. Volume 15(2), pp. 425-431. https://doi.org/10.14716/ijtech.v15i2.6659

Sun, Y., Webley, P. A., 2010. Preparation Of Activated Carbons From Corncob With Large Specific Surface Area By A Variety Of Chemical Activators And Their Application In Gas Storage. *Chemical Engineering Journal,* Volume 162**,** pp. 883-892. https://doi.org/10.1016/j.cej.2010.06.031

Tabak, A., Sevimli, K., Kaya, M., Caglar, B., 2019. Preparation And Characterization Of A Novel Activated Carbon Component Via Chemical Activation Of Tea Woody Stem. *Journal Of Thermal Analysis And Calorimetry,* Volume 138, pp. 3885–3895. https://doi.org/10.1007/s10973-019-08387-2

Titiladunayo, I. F., Mcdonald, A. G. & Fapetu, O. P. 2012. Effect Of Temperature On Biochar Product Yield From Selected Lignocellulosic Biomass In A Pyrolysis Process. *Waste And Biomass Valorization,* Volume 3**,** pp. 311-318. https://doi.org/10.1007/s12649-012-9118-6.

Wulansari, R. & Rezamela, E., 2020. Pengaruh Kompos Limbah Teh Hitam (Tea Fluff) Terhadap Pertumbuhan Benih Teh (Camellia Sinensis (L.) Kuntze). *Jurnal Tanah Dan Sumberdaya Lahan,* Volume 7**,** pp. 341-350. https:10.21776/ub.jtsl.2020.007.2.19

Yek, P. N. Y., Liew, R. K., Osman, M. S., Lee, C. L., Chuah, J. H., Park, Y.-K., Lam, S. S., 2019. Microwave Steam Activation, An Innovative Pyrolysis Approach To Convert Waste Palm Shell Into Highly Microporous Activated Carbon. *Journal Of Environmental Management,* Volume 236**,** pp. 245-253. https://doi.org/10.1016/j.jenvman.2019.01.010

Yıldız, Z., Kaya, N., Topcu, Y., Uzun, H., 2019. Pyrolysis And Optimization Of Chicken Manure Wastes In Fluidized Bed Reactor: CO_2 Capture In Activated Bio-Chars. *Process Safety And Environmental Protection,* Volume 130**,** pp. 297-305. https://doi.org/10.1016/j.psep.2019.08.011

Yuliusman., Putri, S.A., Sipangkar, S.P., Al Farouq, F., Fatkhurrahman, M., 2019. Technology Development of Adsorption Cigarette Smoke using Modified Activated Carbon with MgO from Waste Biomass of Durian Shell. *International Journal of Technology*. Volume 10(8), pp. 1505-1512. https://doi.org/10.14716/ijtech.v10i8.3489

Yuliusman, Purwanto, W.W., Nugroho, Y.S., 2015. Smoke Clearing Method using Activated Carbon and Natural Zeolite. *International Journal of Technology*. Volume 6(3), pp. 492-503. https://doi.org/10.14716/ijtech.v6i3.1125

Zhou, J., Luo, A., Zhao, Y., 2018. Preparation And Characterisation Of Activated Carbon From Waste Tea By Physical Activation Using Steam. *Journal Of The Air & Waste Management Association,* Volume 68**,** pp. 1269-1277. https://doi.org/10.1080/10962247.2018.1460282

Zubbri, N. A., Mohamed, A. R., Lahijani, P., Mohammadi, M., 2021. Low Temperature CO_2 Capture On Biomass-Derived KOH-Activated Hydrochar Established Through Hydrothermal Carbonization With Water-Soaking Pre-Treatment. *Journal Of Environmental Chemical Engineering,* Volume 9**,** pp. 105074. https://doi.org/10.1016/j.jece.2021.105074